LANGMUIR

pubs.acs.org/Langmuir Article

Parameters Affecting Interfacial Assembly and Alignment of Nanotubes

Katherine R. Jinkins, Jonathan H. Dwyer, Anjali Suresh, Sean M. Foradori, Padma Gopalan, and Michael S. Arnold*

Cite This: https://doi.org/10.1021/acs.langmuir.3c02000 Read Online

ACCESS | Metrics & More | Article Recommendations | Supporting Information

ABSTRACT: Tangential flow interfacial self-assembly (TaFISA) is a promising scalable technique enabling uniformly aligned carbon nanotubes for high-performance semiconductor electronics. In this process, flow is utilized to induce global alignment in two-dimensional nematic carbon nanotube assemblies trapped at a liquid/liquid interface, and these assemblies are subsequently deposited on target substrates. Here, we present an observational study of experimental parameters that affect the interfacial assembly and subsequent aligned nanotube deposition. We specifically study the water contact angle (WCA) of the substrate, nanotube ink composition, and water subphase and examine their effects on liquid crystal defects, overall and local alignment, and nanotube bunching or crowding. By varying the substrate chemical functionalization, we determine that highly aligned, densely packed, individualized nanotubes deposit only at relatively small WCA between 35 and 65°. At WCA (< 10°), high nanotube bunching or crowding occurs, and the film is nonuniform, while aligned deposition ceases to occur at higher WCA (>65°). We find that the best alignment, with minimal liquid crystal defects, occurs when the polymer-wrapped nanotubes are dispersed in chloroform at a low (0.6:1) wrapper polymer to nanotube ratio. We also demonstrate that modifying the water subphase through the addition of glycerol not only improves overall alignment and reduces liquid crystal defects but also increases local nanotube bunching. These observations provide important guidance for the implementation of TaFISA and its use toward creating technologies based on aligned semiconducting carbon nanotubes.

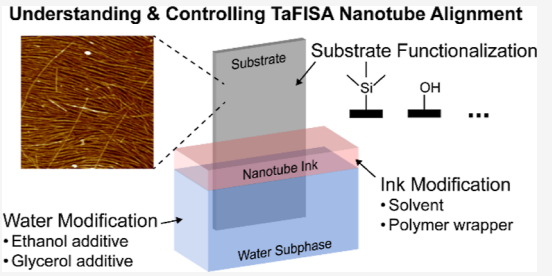

INTRODUCTION

Semiconducting carbon nanotubes are exciting materials for next-generation semiconductor electronics due to their thin body electrostatics, high current carrying capacity, and long mean free paths.[1−3] To exploit the electronic properties of nanotubes in field-effect transistors (FETs), semiconducting carbon nanotubes must be assembled into highly aligned arrays at intermediate (∼100 μm^{-1}) packing densities.[4,5] These ideal nanotube films are predicted to enable FETs with lower power consumption, increased switching speed, and improved electrostatic gating.[4,6−8] However, achieving these ideal films of highly aligned nanotubes has been historically difficult.

Toward producing these ideal films, many techniques have been developed, including shear,[9,10] vacuum filtration,[11] Langmuir−Blodgett[12] and −Schaefer,[13] floating evaporative self-assembly (FESA),[14−16] dimension-limited self-alignment,[17,18] and DNA-directed assembly.[19] Recently, we developed a particularly promising approach—tangential flow interfacial self-assembly (TaFISA)—which results in the deposition of highly aligned nanotube arrays (within ±5.7°) across 10 cm substrates.[20] In this process, an ink of polymer-wrapped nanotubes in organic solvent is flowed through an open channel composed of a target substrate and sacrificial barrier suspended in a water subphase. By translation of the substrate and sacrificial barrier together through the flowing ink/water interface, uniform films of highly aligned nanotubes are fabricated. The high array uniformity translates to excellent FET characteristics and reproducibility with high on-state current density averaging 520 $\mu A\ \mu m^{-1}$ at −0.6 V and FET to FET variation of only 19%.

In this initial work,[20] we determined that the nanotubes collect at the two-dimensional ink/water interface, and the additional confinement at this interface leads to liquid crystal assembly. Due to the underlying liquid crystal phenomena guiding the alignment, increasing ink flow rate, increasing concentration, and decreasing temperature were demonstrated to improve the nanotube alignment. These initial results were promising; however, this previous work primarily focused on elucidating the liquid crystalline mechanism and demonstrating that the aligned nanotube arrays are promising for industrial semiconductor electronics. Here, we present additional

Received: July 16, 2023
Revised: September 11, 2023

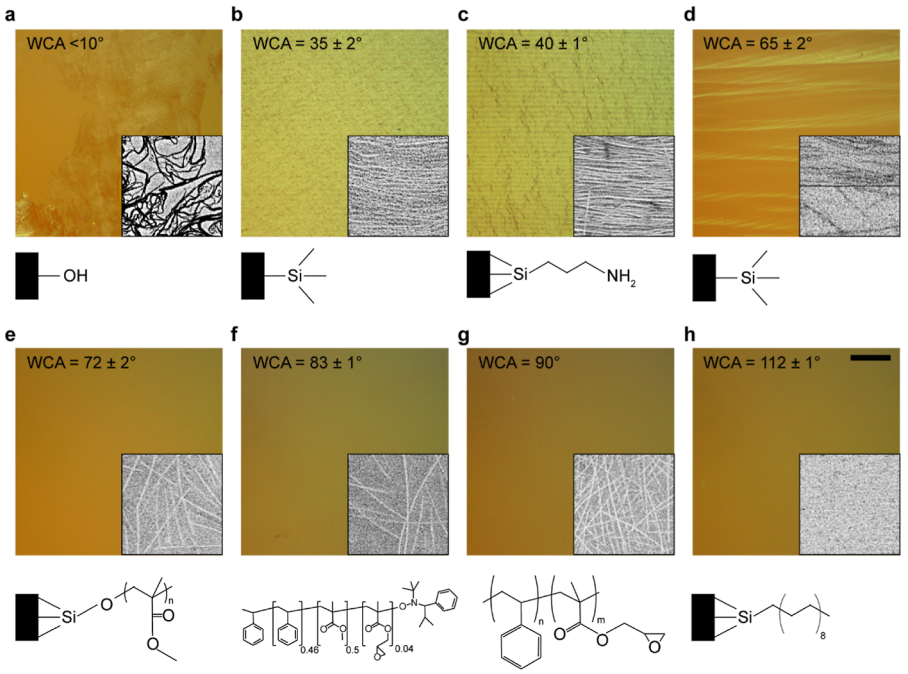

Figure 1. Effect of the chemical functionalization of the substrate surface and WCA on nanotube arrays aligned via TaFISA. (a–h) POM and SEM images (insets) of TaFISA-deposited nanotube arrays on surfaces coated with hydroxyl groups (from piranha treatment) (a), partial HMDS coverage (b), APTES (c), full HMDS coverage (d), surface grafted poly(styrene-*rand*-methyl methacrylate) (PS–PMMA) (e), poly(styrene-*rand*-methyl methacrylate-*rand*-glycidyl methacrylate) (PG4–46) (f), poly(styrene-*rand*-glycidyl methacrylate) (PS-GMA) (g), and OTS (h). Chemical structures of each surface are shown below each respective POM image. Flow direction is horizontal. The SEM insets are 1 × 1 μm^2.

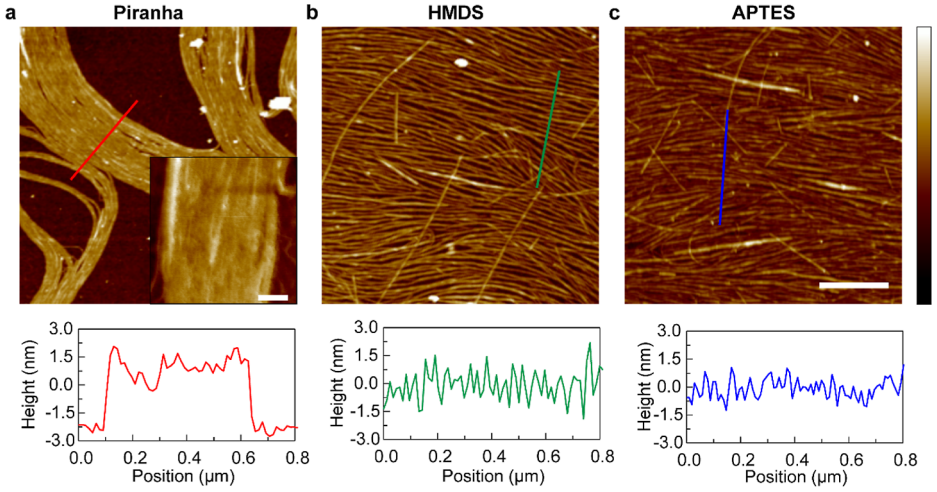

Figure 2. Effect of chemical functionalization of the substrate surface at low WCA on nanotube alignment. (a–c) AFM images and traces of TaFISA nanotube films deposited on piranha, partial HMDS, and APTES-treated substrate surfaces, respectively. Flow direction is horizontal. Color scale bar applies to all panels (range: 10 nm). Linear scale bar in inset in (a) is 60 nm, and linear scale bar in (c) is 500 nm and applies to all large panels.

observations on the effect of deposition parameters, including the substrate, nanotube ink composition (polymer to nanotube ratio and ink solvent), and the water subphase, on the interfacial assembly and subsequent nanotube film morphology (i.e., alignment, nanotube individualization, and liquid crystal defects) from the liquid/liquid interfaces. Preliminary studies of the effect of these parameters on TaFISA have been reported in the thesis of Jinkins.[21] A more thorough report and discussion of these observations are presented here.

EXPERIMENTAL SECTION

Preparation of Poly[(9,9-dioctylfluorenyl-2,7-diyl)-*alt*-*co*-(6,6′-{2,2′-bipyridine})]-Wrapped Semiconducting Carbon Nanotubes. Semiconducting carbon nanotubes are isolated according to our previously published procedures[20] from arc-discharge nanotube soot (Sigma-Aldrich, #698695) using a 1 to 1 ratio by weight of raw soot to polyfluorene derivative polymer wrapper, poly[(9,9-dioctylfluorenyl-2,7-diyl)-*alt*-*co*-(6,6′-{2,2′-bipyridine})] (PFO-BPy) (American Dye Source, Inc., Quebec, Canada; #ADS153-UV). Briefly, PFO-BPy is dispersed in toluene, and this mixture is combined with the nanotube powder at a concentration of 2 mg mL^{-1} and sonicated at 40% amplitude for 30 min using a horn-tip sonicator. The solution is then centrifuged to remove unselected nanotubes and

https://doi.org/10.1021/acs.langmuir.3c02000
Langmuir XXXX, XXX, XXX–XXX

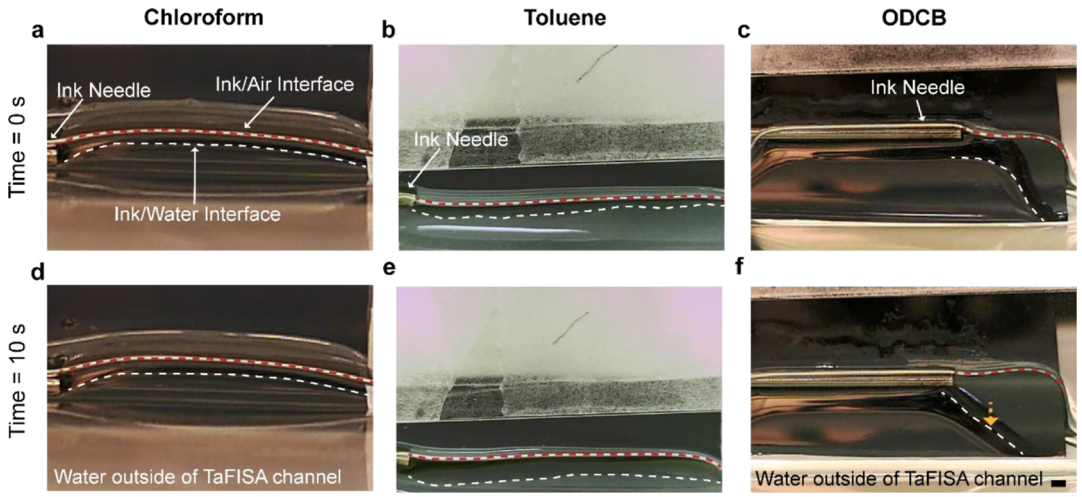

Figure 3. Effect of nanotube ink solvent on ink spreading during TaFISA. Screenshots from video at time = 0 s (i.e., the beginning of the ink flow) (a–c) and time = 10 s (d–f) of TaFISA depositions using nanotube ink with chloroform (a,d), toluene (b,e), and ODCB (c,f) solvents. The ink/water and air/ink interfaces are outlined with dashed white and red lines. Flow direction is horizontal. Scale bar in (f) is 1 mm and applies to all panels.

other amorphous carbon species. The supernatant is collected, and the excess PFO-BPy is removed through subsequent centrifugation and sonication steps until the desired PFO-BPy /nanotube ratio is achieved (3–10 repetitions). The nanotube concentration in the final ink solutions is determined using known optical cross sections from the S_{22} transition.[15,22]

Preparation of Poly[(9,9-dioctylfluorenyl-2,7-diyl)-Wrapped (7,5)-Enriched Semiconducting Carbon Nanotubes. (7,5)-Enriched semiconducting carbon nanotubes are extracted from a CoMoCAT produced small diameter (0.7–1.2 nm) nanotube powder (Southwest Nanotechnologies) using poly(9,9-dioctylfluorene-2,7-diyl) (PFO) following our previously published procedure.[23,24] Briefly, PFO in toluene is combined with CoMoCAT nanotubes (1:0.5 mass ratio) through horn-tip sonication and centrifuged to remove nanotubes not wrapped with the PFO. The excess PFO in the highly pure semiconducting nanotube solution is then removed through subsequent centrifugation and sonication steps to achieve a PFO/nanotube ratio near 1:1.

Preparation of Substrates. Si wafers with 90 nm of dry, thermal oxide, or native oxide are used in this paper. Quartz substrates are also used in Figure 3 as barriers to facilitate viewing of the ink flow dynamics. The substrates are cleaned with a piranha solution of H_2SO_4 (91–92.5%)/H_2O_2 (30%) at a ratio of 2:1 by volume at 110 °C for 1 h, rinsed with deionized water (resistivity ~18 MΩ), and dried with N_2. All substrates except those in Figure 1 and 2 are then baked for 335 s at 205 °C and exposed to 2 s of hexamethyldisilazane (HMDS) vapor. Specific substrate treatment for Figures 1 and 2 and experimental conditions for each figure are included in the Supporting Information (Supporting Note 1).

RESULTS AND DISCUSSION

Effect of Substrate Chemical Functionalization and Water Contact Angle. First, we study the effect of the chemical functionalization of the substrate on the nanotube deposition from inks of arc-discharge semiconducting carbon nanotubes isolated with poly[(9,9-dioctylfluorenyl-2,7-diyl)-*alt*-*co*-(6,6′-{2,2′-bipyridine})] (PFO-BPy) and dispersed in chloroform. Chemical functionalization of the substrate and the sacrificial barrier, which together define the TaFISA channel, can affect the assembly of nanotube films aligned via TaFISA in multiple ways. First, because the TaFISA process relies on a well-formed and controllable ink/water interface and an ink/water/substrate contact line that smoothly moves across the substrate surface, we expect that the water contact angle (WCA) will affect nanotube deposition. For example, if the WCA is too small (i.e., hydrophilic), the ink will not be able to dewet the water from the substrate, and a well-defined ink/water/substrate contact line will not form at the substrate—thereby preventing highly ordered nanotubes from depositing from the 2D nematic assembly at the liquid/liquid interface. Second, the chemical functionalization of the substrate will affect the ability of nanotubes to deposit and adhere to the substrate. Previous work has demonstrated that deposited nanotube density is dependent upon solvent structuring at the substrate, affected by both the chemical functionalization of the target substrate and the nanotube ink solvent.[25] While the original paper reporting the TaFISA process[20] demonstrated uniform and highly aligned nanotubes on surfaces treated with HMDS (WCA = 30–45°), it is important to understand the limitations and effect of the surface chemical functionalization and WCA, independently, toward improving the alignment further.

To study the effect of chemical functionalization on nanotube deposition, substrate and barrier surfaces coated with different self-assembled monolayers and polymers, in which the WCA ranges from less than 10 to 112°, are investigated via scanning electron microscopy (SEM) and polarized optical microscopy (POM) (Figure 1). The optimal nanotube alignment achieved is observed on substrates with partial coverage of HMDS and a corresponding WCA of 35° (Figure 1b) and with 3-aminopropyltriethoxysilane (APTES) and a corresponding WCA of 40° (Figure 1c).

On the other hand, when the WCA is below (WCA < 10°) or above (WCA > 65°), the global nanotube alignment and/or uniformity is worse, and more nanotube bunching can occur. For example, when the WCA is too hydrophobic, several different phenomena are observed. When the WCA is 65°, the deposition results in intermittent regions of highly aligned nanotubes (Figure 1d) due to the ink/water interface stick–slipping across the substrate. At higher WCAs between 72 and 90° (Figure 1e–g), only random nanotube films of various densities are deposited on the substrate, likely from the bulk of the nanotube ink (i.e., not from the ink/water interface). Nanotubes depositing from the bulk of the ink are also likely the cause of the crossing nanotubes deposited on the aligned

https://doi.org/10.1021/acs.langmuir.3c02000
Langmuir XXXX, XXX, XXX–XXX

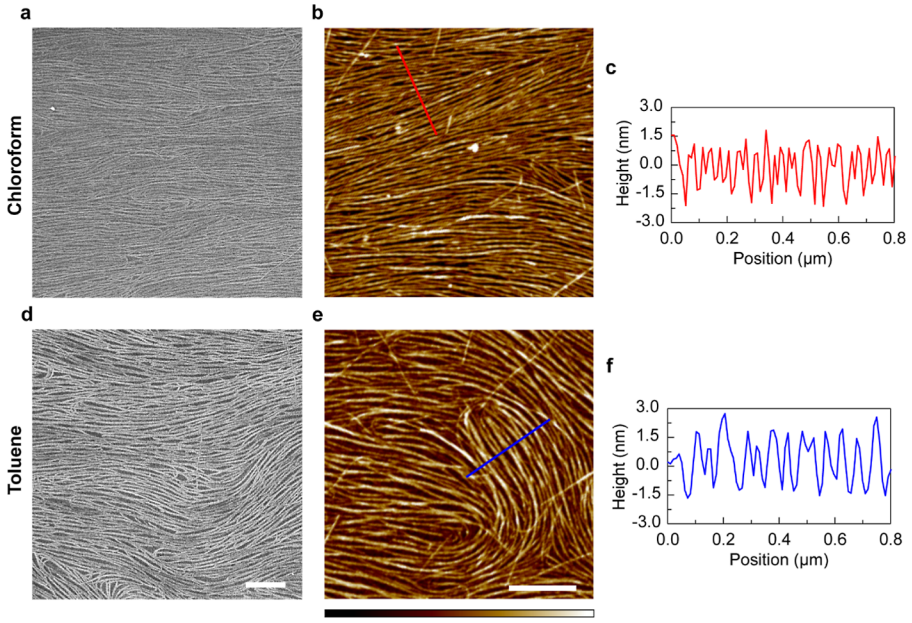

Figure 4. Effect of the nanotube ink solvent on TaFISA-aligned nanotube arrays. SEM image, AFM image, and AFM cross-section from TaFISA films obtained using nanotube inks with chloroform (a–c) and toluene (d–f) as the organic solvent, respectively. Flow direction is horizontal. The scale bar in (d) is 500 nm and applies to (a,d). Linear scale bar in (e) is 500 nm, and color bar range below is 6 nm. Both scale bars apply to (b,e).

arrays shown in Figure 1c inset as well as similar aligned films throughout the paper. At an even higher WCA of 112° on a surface terminated with octadecyltrichlorosilane (OTS), nanotubes are not deposited at all. Future experiments will be needed to explore mechanisms in more detail, but the lack of alignment of the nanotubes at WCAs greater than 65° is hypothesized to be due to irregularities in the movement of the ink/water contact line. The density dependence observed in Figure 1e–h can likely be attributed to varying nanotube adhesion to the substrate as a result of different solvent structuring, as demonstrated by Dwyer et al.[25]

In contrast, when the substrate surface is too hydrophilic (WCA < 10°), which is achieved by functionalizing the surface with hydroxyl groups via piranha treatment, the nanotubes deposit in noncontinuous bunched arrays with high local alignment (Figure 2a). This bunching likely occurs because the water subphase does not dewet from the substrate, inhibiting formation of a well-defined, linear substrate/ink/water contact line and interfering with nanotube deposition from the ink/water interface onto the substrate. The films are noncontinuous and lack global alignment; however, high nanotube packing densities are achieved (>100 μm^{-1}, inset in Figures 2a and S1) due to nanotube bunching. Even though the nanotubes are bunched laterally, their thickness (3 nm) is consistent with that of approximately one to two layers of polymer-wrapped nanotubes. In comparison, the atomic force microscopy (AFM) data show that the HMDS- and APTES-functionalized substrates demonstrate very similar array morphology including similar nanotube packing densities, 51 ± 5 and 56 ± 8 μm^{-1}, respectively, despite the difference in functional headgroup termination (methyl versus amine) (Figure 2b,c). For the remainder of this paper, we use HMDS-treated substrates with a WCA of 35°.

Effect of Solvent and Wrapping Polymer on TaFISA Alignment. To elucidate the effect of ink solvent on resulting nanotube deposition, we first study the effect of ink solvent on ink spreading and the water/solvent/substrate contact line (Figure 3). We compare nanotube ink composed of polymer-wrapped nanotubes and three separate solvents: chloroform, toluene, and 1,2-orthodichlorobenzene (ODCB) flowed through a TaFISA channel on a water subphase (schematic of the experimental setup shown in Figure S2). The chloroform and toluene inks are composed of arc-discharge semiconducting carbon nanotubes isolated with PFO-BPy, while the ODCB ink is composed of (7,5)-enriched nanotubes isolated with poly[(9,9-dioctylfluorenyl-2,7-diyl) (PFO) from as-produced cobalt molybdenum catalysis of carbon monoxide disproportionation (CoMoCAT) powder.

After injecting ink into the channel (i.e., at time = 10 s), chloroform and toluene ink form thin ink layers on the water that are 1.0 ± 0.1 mm (Figure 3d) and 1.6 ± 0.2 mm (Figure 3e) thick, respectively, while the ODCB forms a thicker layer with larger variation, 5.0 ± 2.0 mm. Additionally, instead of flowing across the channel length, the ink flows downward (Figure 3f). This difference in flow dynamics is likely due to rheological differences, including solvent density, viscosity, and interfacial energies. For example, solvent density will influence whether the ink is supported on top of water (ρ = 1 g mL^{-1}) or sinks. The density of toluene is 0.9 g mL^{-1} which is favorable for layering on top of the water, while the densities of ODCB and chloroform are 1.3 and 1.5 g mL^{-1}, respectively, decreasing the ability of these inks to flow through the TaFISA channel before sinking. However, previous work has shown that the ethanol stabilizer used in the chloroform leads to fast spreading of chloroform on water,[14,16] which may help the chloroform ink flow through the channel before dropping, unlike ODCB. The flow will also be influenced by the spreading parameter, S, which is based on the air–water surface tension, the air–oil surface tension, and the oil–water interfacial tension. When S is positive, the oil will spread over water, while for a negative S, oil will not spread on the water as it is not energetically favorable. For chloroform–water and toluene–water, $S > 0$ (see Supporting Information Note 2 for calculation), while for

https://doi.org/10.1021/acs.langmuir.3c02000
Langmuir XXXX, XXX, XXX–XXX

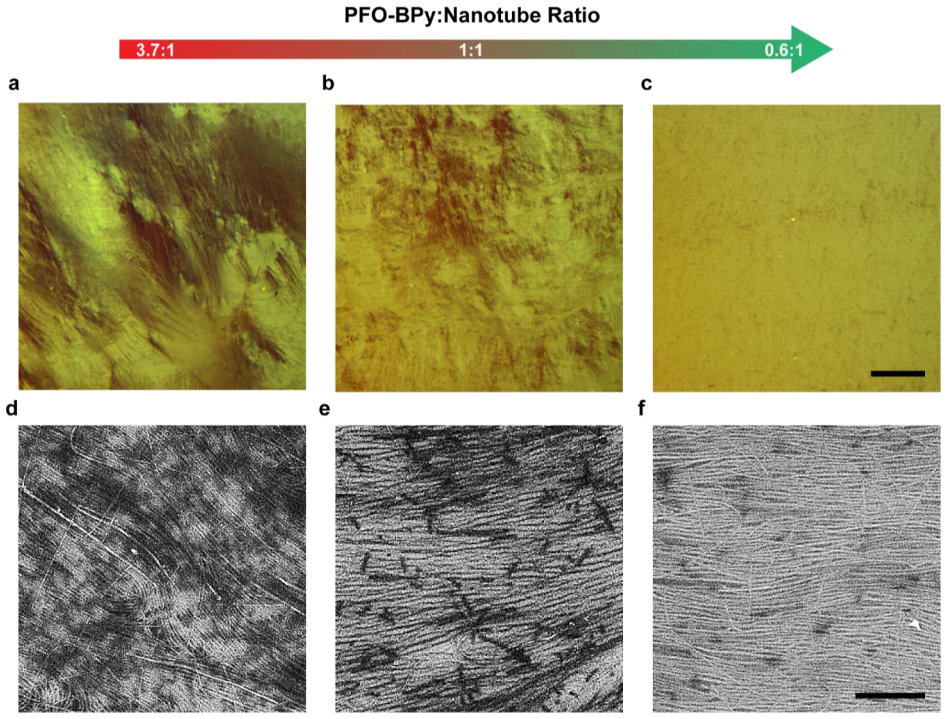

Figure 5. Effect of the PFO-BPy to nanotube ratio on nanotube arrays aligned via TaFISA. (a–c) POM images from TaFISA films fabricated using nanotube ink with PFO-BPy/nanotube ratios of 3.7:1, 1:1, and 0.6:1, respectively. Flow direction is horizontal. Scale bar in (c) is 250 μm and applies to (a–c). (d–f) SEM images of TaFISA films shown in (a–c), respectively. Scale bar in (f) is 500 nm and applies to (d–f).

ODCB–water, S is negative,[26,27] inhibiting controllable nanotube deposition from the TaFISA process.

The solvent viscosities are also different, which likely influences the ink spreading. Toluene and chloroform have similar viscosities of 0.6 mPa S, while the viscosity of the ODCB is 1.3 mPa S. Increased ink viscosity will reduce the ink velocity, in turn decreasing the likelihood of the ink flowing through the channel before pooling and sinking.

We study in more detail the resulting nanotube alignment from using the two solvents with more controlled deposition dynamics—chloroform and toluene. SEM and AFM images of nanotube arrays aligned via TaFISA using chloroform and toluene are shown in Figure 4. While both solvents result in locally aligned nanotube arrays, SEM and AFM of the depositions show more waviness and deviation from the flow direction in the toluene deposition (Figure 4d,e). The toluene ink layer thickness increases more over time (110% increase) at the same ink flow rate and channel width as chloroform (10% increase) (Figure 3); thus, this lower degree of alignment could be partly caused by lower effective shear rates in the channel. AFM also indicates that in the toluene deposition, the nanotubes are more bunched on the substrate (resulting in wider traces in the AFM section). The lower solubility of nanotubes within the toluene ink could be an additional cause of bunching within the film.

Regardless of the solvent (chloroform, toluene, or ODCB), aligned nanotube arrays are formed (Figures 4, S3), which are characteristic of the two-dimensional interfacial assembly of TaFISA. This indicates that the interfacial assembly is not restricted to the PFO-BPy-wrapped arc-discharge nanotubes in chloroform used in our previous work and can be adapted to different combinations of solvents and polymer wrappers and to nanotubes produced via different methods. However, the ODCB ink deposition is very nonuniform with only a thin layer of aligned nanotube aggregates at the top of the deposition area (Figure S3). While the smaller diameter (7,5) nanotubes (diameter of 0.82 nm) in the ODCB ink are less stiff and will be more difficult to align than arc-discharge nanotubes (diameter ~1.5 nm) in the chloroform and toluene inks, the large nonuniformity across the film is likely due to poor spreading of the ink layer (Figure 3c,f). For the remainder of this article, we use inks of PFO-BPy-wrapped arc-discharge nanotubes dispersed in chloroform.

Effect of PFO-BPy Wrapping Polymer to Nanotube Ratio. Because the TaFISA process relies on the interfacial adsorption of nanotubes at the ink/water interface, we expect that the amount of free polymer in the solution will affect the alignment and morphology of the resulting nanotube films. Here, we observe that decreasing the PFO-BPY/ nanotube ratio results in more uniform nanotube arrays, with smaller defected regions and less deviation from the flow direction (Figure 5). This trend is qualitatively observed from POM images at three different PFO-BPy/nanotube ratios, where brighter yellow indicates that the nanotubes are aligned with the flow direction (horizontal) and darker regions correspond to nanotubes misaligned from the direction of flow. At a high PFO-BPy/nanotube ratio of 3.7:1, the POM image exhibits some bright yellow regions; however, a large portion of the image shows dark regions, where the nanotube alignment is changing direction. At a ratio of 1:1, the darker defective regions where the alignment is changing direction become smaller, and at a much lower ratio of 0.6:1, the film is almost uniformly yellow, indicating that the majority of the nanotubes are aligned with the direction of flow. The small dark regions observed in Figure 5c are small deviations in alignment and have been correlated primarily to liquid crystal defects due to the underlying role of liquid crystal assembly on alignment.[20] The effect of the PFO-BPy/nanotube ratio is also seen on a

https://doi.org/10.1021/acs.langmuir.3c02000
Langmuir XXXX, XXX, XXX–XXX

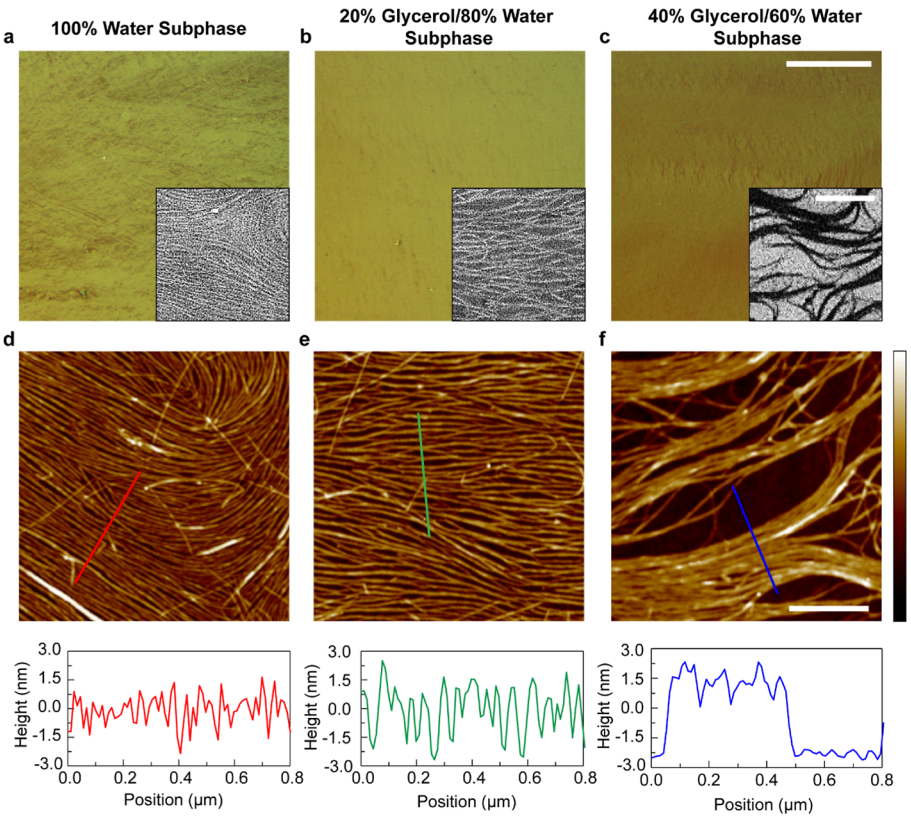

Figure 6. Effect of the addition of glycerol in the water subphase on nanotube films aligned via TaFISA. POM and SEM (inset) images of nanotube films obtained using all water subphase (a), a subphase of 20 vol % glycerol and 80 vol % water (b), and a subphase of 40 vol % glycerol and 60 vol % water (c) at a flow rate of 0.5 mL min^{-1}. Flow direction is horizontal. Scale bars in (c) are 250 μm (POM image) and 500 nm (SEM image) and apply to (a–c). (d–f) AFM and traces (below) of aligned nanotube morphology using the subphases in (a–c), respectively, at a flow rate of 1 mL min^{-1}. Scale bar in (f) is 500 nm and color bar range at right is 9.5 nm, and both apply to (d–f).

more local scale in SEM images Figure 5d–f. With a decreasing PFO-BPy/nanotube ratio, the nanotube alignment becomes more oriented with the direction of flow, consistent with the POM data. Additionally, at high polymer ratios, more black "spots" are seen on the film, which correspond to free PFO-BPy (i.e., polymer that is not wrapping a nanotube but instead is free in the solution) that deposits from the solution along with the nanotubes and can be removed by refluxing in toluene (shown in Figure S4). The amount of free polymer deposited on the nanotube films decreases with decreasing PFO-BPy/nanotube ratio.

These results indicate that to achieve uniform films of highly aligned nanotubes from the TaFISA technique, a low polymer to nanotube ratio must be used. However, if the PFO-BPy/nanotube ratio is too low, the nanotubes will aggregate in the solution, so likely that there is an intermediate range of ideal PFO-BPy/nanotube concentrations. AFM measurements of individual nanotubes (Figure S5) show that the average nanotube heights are consistent across the PFO-BPy/nanotube ratio range studied here, indicating that the improvement in film uniformity and alignment observed is not due to changes of the individual nanotube aggregation within the inks.

Effect of Water Subphase Modification. Formation of a well-defined ink/water interface and ink/water/substrate contact line is paramount for collecting and confining the nanotubes into nematic assemblies, aligning the nanotubes with flow, and depositing the aligned nanotubes onto the target substrate without disorder. With the goal of obtaining a more controlled ink/water interface, we studied the effect of an additive with high viscosity, glycerol (μ = 1500 mPa S), on the water subphase (Figure 6). POM images from TaFISA depositions using subphases consisting of 100% water (Figure 6a), 20% glycerol/80% water (by volume) (Figure 6b), and 40% glycerol/60% water (by volume) (Figure 6c) are shown at a volumetric flow rate of 0.5 mL min^{-1}. The addition of glycerol will also slightly lower the water surface tension,[28] however, not substantially enough to prevent an ink/water interface and the resulting 2D nanotube liquid crystals from forming. With the addition of 20% glycerol to the water subphase, the POM images of the nanotube film are globally uniform, with less defected regions (Figure 6b compared to Figure 6a, deposition without glycerol); however, with the addition of 40% glycerol, the POM images are darker and less homogeneous, indicating more disordered nanotube alignment (Figure 6c). The POM uniformity with an intermediate amount of glycerol added to the water subphase is promising; however, comparison of the SEM insets from depositions (Figure 6a,b,c) and AFM measurements (Figure 6d,e,f) shows that the addition of glycerol increases the nanotube bunching while at the same time marginally increasing the thickness of the nanotube layer, indicating multilayers or a small degree of bundling. While individualized nanotubes are thought to be more desirable, bundled nanotubes may still be sufficient for high-performance devices as recent work demonstrated high transconductance and current densities in FETs based on arrays of bundled nanotubes.[29] Future work will focus on taking advantage of subphase modification to increase nanotube alignment and uniformity while also preventing

https://doi.org/10.1021/acs.langmuir.3c02000
Langmuir XXXX, XXX, XXX–XXX

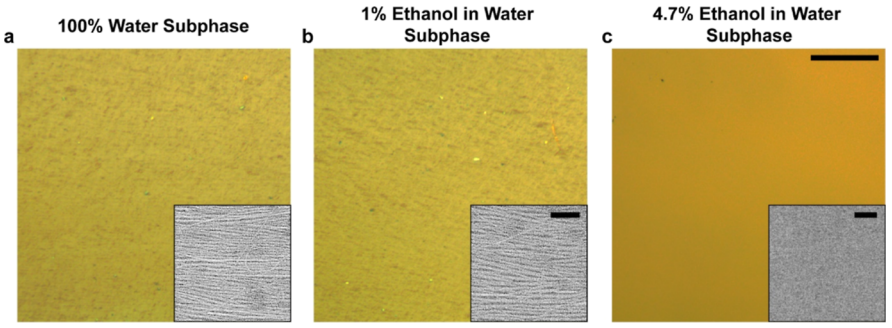

Figure 7. Effect of ethanol in the water subphase. (a–c) POM and SEM (inset) images obtained from TaFISA depositions with 0, 1, and 4.7 vol % ethanol in the water subphase, respectively. The large scale bar in (c) is 200 μm and applies to POM images in (a–c). Flow direction is horizontal. The scale bar in the SEM inset in (b) is 250 nm and applies to parts (a) and (b). The scale bar in the SEM inset in (c) is 1 μm.

deleterious nanotube aggregation into larger bundles (>5 nm in size) that are more difficult to electrostatically gate.[29]

We also investigate the effect of ethanol in the water subphase to study how decreasing the subphase surface tension affects the TaFISA alignment. Through previous work, we have determined that the ethanol stabilizer (as opposed to the amylene stabilizer) in chloroform is vital to achieve alignment in FESA films.[16] With 1 vol % ethanol in the water subphase (Figure 7b), the nanotube films are very similar to films obtained with a 100% water subphase (Figure 7a). However, with 4.7 vol % ethanol in the water subphase, nanotubes are not deposited onto the substrate (Figure 7b) at all. While videos of ink spreading and contact-line dynamics during these depositions with different ethanol concentrations look similar, at 4.7 vol % ethanol, we hypothesize that the surface tension of the water is sufficiently decreased to interfere with the accumulation of nanotubes at the liquid/liquid interface.

CONCLUSIONS

In this work, we perform more detailed studies into experimental parameters that directly affect the interfacial assembly and alignment of carbon nanotubes in the TaFISA process. We find that the interfacial assembly of carbon nanotubes occurs for at least two types of carbon nanotubes and polymer wrappers—arc-discharge and (7,5)-enriched nanotubes from the CoMoCAT process, wrapped with PFO-BPy and PFO, respectively. We optimized the PFO-BPy/nanotube ratio to obtain highly aligned nanotube films at a 0.6:1 ratio. Furthermore, we identify the window of the substrate WCA over which optimum carbon nanotube alignment occurs. Modification of the water subphase is studied through the addition of glycerol and ethanol. The alignment on a glycerol/water subphase is promising for future investigations due to the high macroscopic film uniformity and alignment and could be especially promising if used in conjunction with a polymer wrapper that more strongly prevents bundling of nanotubes. Additionally, future work would also need to be performed to determine if glycerol residues remain on the nanotubes and how the residues affect the device performance. This work demonstrates important progress toward determining the parameter space that affects the liquid–liquid interfacial assembly of nanotubes.

ASSOCIATED CONTENT

Supporting Information

The Supporting Information is available free of charge at https://pubs.acs.org/doi/10.1021/acs.langmuir.3c02000.

Experimental parameters for each figure; AFM image of Figure 2a inset; schematic of the TaFISA experimental setup and camera placement; spreading parameters for toluene, chloroform, and ODCB; SEM images of TaFISA using ODCB; SEM of the effect of toluene refluxing to remove excess polymer; and AFM of spuncast nanotubes from inks with different polymer concentrations (PDF)

AUTHOR INFORMATION

Corresponding Author

Michael S. Arnold − *Department of Materials Science and Engineering, University of Wisconsin-Madison, Madison, Wisconsin 53706, United States*; Email: michael.arnold@wisc.edu

Authors

Katherine R. Jinkins − *Department of Materials Science and Engineering, University of Wisconsin-Madison, Madison, Wisconsin 53706, United States*; orcid.org/0000-0001-5757-1136

Jonathan H. Dwyer − *Department of Chemical and Biological Engineering, University of Wisconsin−Madison, Madison, Wisconsin 53706, United States*

Anjali Suresh − *Department of Materials Science and Engineering, University of Wisconsin-Madison, Madison, Wisconsin 53706, United States*

Sean M. Foradori − *Department of Materials Science and Engineering, University of Wisconsin-Madison, Madison, Wisconsin 53706, United States*; orcid.org/0000-0002-9142-556X

Padma Gopalan − *Department of Materials Science and Engineering, University of Wisconsin-Madison, Madison, Wisconsin 53706, United States; Department of Chemistry, University of Wisconsin−Madison, Madison, Wisconsin 53706, United States*; orcid.org/0000-0002-1955-640X

Complete contact information is available at: https://pubs.acs.org/10.1021/acs.langmuir.3c02000

Author Contributions

All authors contributed in preparing the manuscript.

Notes

The authors declare the following competing financial interest(s): K.R.J. and M.S.A. are co-founders of SixLine Semiconductor, Inc., which aims to commercialize aligned semiconducting carbon nanotube electronics. P.G. is also a technical advisor to SixLine Semiconductor, Inc.

https://doi.org/10.1021/acs.langmuir.3c02000
Langmuir XXXX, XXX, XXX−XXX

■ ACKNOWLEDGMENTS

This work was supported by the NSF-SNM award no. 1727523 (K.R.J., J.H.D., A.S., P.G., M.S.A.). K.R.J. furthermore acknowledges support from the NSF Graduate Research Fellowship Program, award no. DGE-1256259 and the University of Wisconsin Distinguished Graduate Fellowship. Support is also acknowledged from the Office of Naval Research Award no. N00014-22-1-2843 (S.M.F., M.S.A.). The authors gratefully acknowledge the use of facilities and instrumentation supported by NSF through the University of Wisconsin Materials Research Science and Engineering Center (DMR-1121288, 0079983, and 0520057) and through the University of Wisconsin Nanoscale Science and Engineering Center (DMR-0832760 and 0425880).

■ REFERENCES

(1) Cao, Q.; Tersoff, J.; Farmer, D. B.; Zhu, Y.; Han, S.-J. Carbon Nanotube Transistors Scaled to a 40-Nanometer Footprint. *Science* **2017**, *356* (6345), 1369−1372.
(2) Avouris, P.; Appenzeller, J.; Martel, R.; Wind, S. J. Carbon Nanotube Electronics. *Proc. IEEE* **2003**, *9* (11), 1772−1784.
(3) Javey, A.; Guo, J.; Wang, Q.; Lundstrom, M.; Dai, H. Ballistic Carbon Nanotube Field-Effect Transistors. *Nature* **2003**, *424* (6949), 654−657.
(4) Tulevski, G. S.; Franklin, A. D.; Frank, D.; Lobez, J. M.; Cao, Q.; Park, H.; Afzali, A.; Han, S.-J.; Hannon, J. B.; Haensch, W. Toward High-Performance Digital Logic Technology with Carbon Nanotubes. *ACS Nano* **2014**, *8* (9), 8730−8745.
(5) Rutherglen, C.; Jain, D.; Burke, P. Nanotube Electronics for Radiofrequency Applications. *Nat. Nanotechnol.* **2009**, *4* (12), 811−819.
(6) Franklin, A. D.; Luisier, M.; Han, S.-J.; Tulevski, G.; Breslin, C. M.; Gignac, L.; Lundstrom, M. S.; Haensch, W. Sub-10 Nm Carbon Nanotube Transistor. *Nano Lett.* **2012**, *12* (2), 758−762.
(7) Qiu, C.; Zhang, Z.; Xiao, M.; Yang, Y.; Zhong, D.; Peng, L.-M. Scaling Carbon Nanotube Complementary Transistors to 5-Nm Gate Lengths. *Science* **2017**, *355* (6322), 271−276.
(8) Franklin, A. D.; Hersam, M. C.; Wong, H.-S. P. Carbon Nanotube Transistors: Making Electronics from Molecules. *Science* **2022**, *378* (6621), 726−732.
(9) Jinkins, K. R.; Chan, J.; Jacobberger, R. M.; Berson, A.; Arnold, M. S. Substrate-Wide Confined Shear Alignment of Carbon Nanotubes for Thin Film Transistors. *Adv. Electron. Mater.* **2019**, *5* (2), 1800593.
(10) Tune, D. D.; Stolz, B. W.; Pfohl, M.; Flavel, B. S. Dry Shear Aligning: A Simple and Versatile Method to Smooth and Align the Surfaces of Carbon Nanotube Thin Films. *Nanoscale* **2016**, *8* (6), 3232−3236.
(11) He, X.; Gao, W.; Xie, L.; Li, B.; Zhang, Q.; Lei, S.; Robinson, J. M.; Hároz, E. H.; Doorn, S. K.; Wang, W.; Vajtai, R.; Ajayan, P. M.; Adams, W. W.; Hauge, R. H.; Kono, J. Wafer-Scale Monodomain Films of Spontaneously Aligned Single-Walled Carbon Nanotubes. *Nat. Nanotechnol.* **2016**, *11* (7), 633−638.
(12) Li, X.; Zhang, L.; Wang, X.; Shimoyama, I.; Sun, X.; Seo, W.-S.; Dai, H. Langmuir-Blodgett Assembly of Densely Aligned Single-Walled Carbon Nanotubes from Bulk Materials. *J. Am. Chem. Soc.* **2007**, *129* (16), 4890−4891.
(13) Sgobba, V.; Giancane, G.; Cannoletta, D.; Operamolla, A.; Hassan Omar, O.; Farinola, G. M.; Guldi, D. M.; Valli, L. Langmuir-Schaefer Films for Aligned Carbon Nanotubes Functionalized with a Conjugate Polymer and Photoelectrochemical Response Enhancement. *ACS Appl. Mater. Interfaces* **2014**, *6* (1), 153−158.
(14) Jinkins, K. R.; Chan, J.; Brady, G. J.; Gronski, K. K.; Gopalan, P.; Evensen, H. T.; Berson, A.; Arnold, M. S. Nanotube Alignment Mechanism in Floating Evaporative Self-Assembly. *Langmuir* **2017**, *33* (46), 13407−13414.
(15) Brady, G. J.; Way, A. J.; Safron, N. S.; Evensen, H. T.; Gopalan, P.; Arnold, M. S. Quasi-Ballistic Carbon Nanotube Array Transistors with Current Density Exceeding Si and GaAs. *Sci. Adv.* **2016**, *2* (9), No. e1601240.
(16) Joo, Y.; Brady, G. J.; Arnold, M. S.; Gopalan, P. Dose-Controlled, Floating Evaporative Self-Assembly and Alignment of Semiconducting Carbon Nanotubes from Organic Solvents. *Langmuir* **2014**, *30* (12), 3460−3466.
(17) Liu, L.; Han, J.; Xu, L.; Zhou, J.; Zhao, C.; Ding, S.; Shi, H.; Xiao, M.; Ding, L.; Ma, Z.; Jin, C.; Zhang, Z.; Peng, L.-M. Aligned, High-Density Semiconducting Carbon Nanotube Arrays for High-Performance Electronics. *Science* **2020**, *368* (6493), 850−856.
(18) Shi, H.; Ding, L.; Zhong, D.; Han, J.; Liu, L.; Xu, L.; Sun, P.; Wang, H.; Zhou, J.; Fang, L.; Zhang, Z.; Peng, L.-M. Radiofrequency Transistors Based on Aligned Carbon Nanotube Arrays. *Nat. Electron.* **2021**, *4* (6), 405−415.
(19) Zhao, M.; Chen, Y.; Wang, K.; Zhang, Z.; Streit, J. K.; Fagan, J. A.; Tang, J.; Zheng, M.; Yang, C.; Zhu, Z.; Sun, W. DNA-Directed Nanofabrication of High-Performance Carbon Nanotube Field-Effect Transistors. *Science* **2020**, *368* (6493), 878−881.
(20) Jinkins, K. R.; Foradori, S. M.; Saraswat, V.; Jacobberger, R. M.; Dwyer, J. H.; Gopalan, P.; Berson, A.; Arnold, M. S. Aligned 2D Carbon Nanotube Liquid Crystals for Wafer-Scale Electronics. *Sci. Adv.* **2021**, *7* (37), No. eabh0640.
(21) Jinkins, K. R. Wafer-Scale Alignment of Semiconducting Carbon Nanotubes from Solution, Ph. D. Thesis, The University of Wisconsin: Madison, United States, Wisconsin, 2020. (accessed 2023−09−11). https://www.proquest.com/docview/2624647156/abstract/EE1F8D325FA4C05PQ/1.
(22) Mistry, K.; Larsen, B.; Blackburn, J. High-Yield Dispersions of Large-Diameter Semiconducting Single-Walled Carbon Nanotubes with Tunable Narrow Chirality Distributions. *ACS Nano* **2013**, *7* (3), 2231−2239.
(23) Shea, M. J.; Arnold, M. S. 1% Solar Cells Derived from Ultrathin Carbon Nanotube Photoabsorbing Films. *Appl. Phys. Lett.* **2013**, *102* (24), 243101.
(24) Wang, J.; Shea, M. J.; Flach, J. T.; McDonough, T. J.; Way, A. J.; Zanni, M. T.; Arnold, M. S. Role of Defects as Exciton Quenching Sites in Carbon Nanotube Photovoltaics. *J. Phys. Chem. C* **2017**, *121* (15), 8310−8318.
(25) Dwyer, J. H.; Shen, Z.; Jinkins, K. R.; Wei, W.; Arnold, M. S.; Van Lehn, R. C.; Gopalan, P. Solvent-Mediated Affinity of Polymer-Wrapped Single-Walled Carbon Nanotubes for Chemically Modified Surfaces. *Langmuir* **2019**, *35* (38), 12492−12500.
(26) Zhang, Z.; Li, H.; Miller, R.; Malissa, H.; Jamali, S.; Boehme, C.; Grossman, J. C.; Ren, S. Freestanding Organic Charge-Transfer Conformal Electronics. *Nano Lett.* **2018**, *18* (7), 4346−4354.
(27) Noh, J.; Jeong, S.; Lee, J.-Y. Ultrafast Formation of Air-Processable and High-Quality Polymer Films on an Aqueous Substrate. *Nat. Commun.* **2016**, *7* (1), 12374.
(28) Takamura, K.; Fischer, H.; Morrow, N. R. Physical Properties of Aqueous Glycerol Solutions. *J. Pet. Sci. Eng.* **2012**, *98−99*, 50−60.
(29) Foradori, S. M.; Dwyer, J. H.; Suresh, A.; Gopalan, P.; Arnold, M. S. High Transconductance and Current Density in Field Effect Transistors Using Arrays of Bundled Semiconducting Carbon Nanotubes. *Appl. Phys. Lett.* **2022**, *121* (7), 073504.

https://doi.org/10.1021/acs.langmuir.3c02000
Langmuir XXXX, XXX, XXX−XXX